JOURNAL OF MATERIALS SCIENCE 23 (1988) 329–331

Hydrogen absorption and desorption in Nd_2Fe_{17} and Sm_2Fe_{17}

WANG XIANG-ZHONG, K. DONNELLY, J. M. D. COEY
Physics Department, Trinity College, Dublin 2, Ireland

B. CHEVALIER, J. ETOURNEAU, T. BERLUREAU
Laboratorie de Chimie du Solide du CNRS, 351 Cours de la Liberation, 33405 Talence, France

The uptake of hydrogen by Nd_2Fe_{17} and Sm_2Fe_{17} has been monitored in a thermopiezic analyser as a function of temperature at an initial pressure of 1 bar (10^5 Pa). The first stage of hydrogen absorption around 250° C yields $R_2Fe_{17}H_y$ (R = Nd, Sm) with $y \simeq 2.2$; this compound retains the Th_2Zn_{17} structure of the starting alloy but the cell volume is increased by about 3%. The Curie temperature increases from 57 to 175° C for R = Nd and from 115 to 253° C for R = Sm. A second stage of hydrogen absorption at about 600° C corresponds to disproportionation of the alloy into α-Fe + $RH_{2-\varepsilon}$.

1. Introduction

Iron-rich intermetallic compounds with rare-earth elements are usually ferromagnetic, with a relatively low Curie temperature. For example, T_c for Y_2Fe_{17} is 51° C, whereas T_c is 913° C for the isomorphic cobalt compound Y_2Co_{17} [1]. The low Curie temperatures of the R_2Fe_{17} series (where R = rare earth) preclude their use as permanent magnets [2]. Furthermore, the pressure coefficient (dT_c/dP) for Y_2Fe_{17} is large and negative, $-5.0\,K\,kbar^{-1}$ ($-5.0 \times 10^{-8}\,K\,Pa^{-1}$) [3]. This suggests that the shorter iron–iron distances are associated with weaker ferromagnetic (or even antiferromagnetic) coupling, in agreement with the Slater–Néel curve.

More recently, it has been shown that hydrogen will dramatically increase the ordering temperature of amorphous Fe_xY_{1-x} alloys with $x \gtrsim 0.7$ [4, 5]. A less marked effect, with $(1/T_c)(dT_c/dy) = 5\%$, has been reported in $Y_2Fe_{14}BH_y$ [6] and other compounds with the $Nd_2Fe_{14}B$ structure [7–9].

Surprisingly, there seem to be no reports in the literature of the effect of hydrogen on the magnetic properties of R_2Fe_{17} compounds, although the hydrogenation behaviour of Sm_2Co_{17} and Pr_2Co_{17} has been studied [10]. R_2Fe_{17} is the most iron-rich intermetallic phase with the rare earths, and in view of the large negative pressure coefficient of T_c, one might expect a substantial increase on hydrogenation if $R_2Fe_{17}H_y$ phases can be prepared. In this paper we report just such an effect for compounds with the light rare earths R = Nd, Sm. Nd_2Fe_{17} and Sm_2Fe_{17} have the rhombohedral Th_2Zn_{17} structure (space group $R\bar{3}m$), which is related to that of the permanent-magnet alloy $SmCo_5$. We monitor the hydrogen uptake of the R_2Fe_{17} compounds and compare results with those of $R_2Fe_{14}B$.

2. Sample preparation and hydrogenation

Nd_2Fe_{17} and Sm_2Fe_{17} were prepared by arc-melting the 99.9% pure elements under argon with a 5% excess of the rare earth, and then annealing for a week at 900° C in quartz tubes sealed under vacuum. The products were examined by X-ray diffraction using $CuK\alpha$ radiation. The neodymium alloy consisted of the pure Th_2Zn_{17}-structure phase, whereas the samarium alloy also contained traces of α-Fe. Lattice parameters determined by using a silicon internal standard are given in Table I. The X-ray diagrams were indexed on a hexagonal cell containing three formula units. Values of a and c are in agreement with earlier determinations [11].

The samples of the alloys ($\simeq 50$ mg) were hydrogenated in the thermopiezic analyser (TPA) shown schematically in Fig. 1. The pressure is continuously monitored in a $1.6\,cm^3$ enclosed volume, a small portion of which is occupied by the sample mounted in a quartz tube of 2 mm internal diameter, which is heated in a programmable furnace [12].

A typical TPA trace for Nd_2Fe_{17}, showing the temperature dependence of the hydrogen pressure and its derivative, is shown in Fig. 2. There are two distinct steps in the curve that closely resemble those found

TABLE I Properties of compounds studied

Compound	a (nm)	c (nm)	$\Delta V/V$ (%)	T_c (° C)	M_s (μ_B per formula) at 20° C	$\langle B_{hf} \rangle$ (T) at 20° C
Nd_2Fe_{17}	0.8578	1.2462	2.8	57	22.9	16.9
$Nd_2Fe_{17}H_{2.4}$	0.8681	1.2510		175	30.9	22.9
Sm_2Fe_{17}	0.8553	1.2442	2.9	115	23.2	22.3
$Sm_2Fe_{17}H_{2.0}$	0.8653	1.2506		253	31.3	25.5

0022-2461/88 $03.00 + .12 © *1988 Chapman and Hall Ltd.*

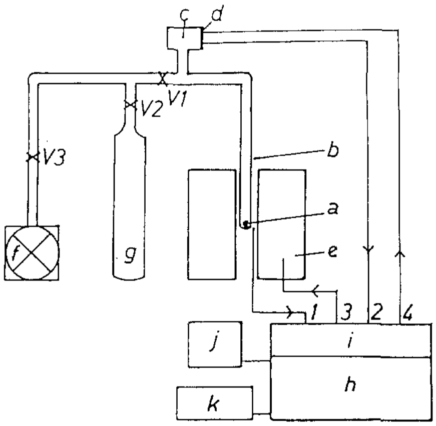

Figure 1 Schematic diagram of the thermopiezic analyser (TPA). (a) Sample, (b) sample tube, (c) chamber, (d) pressure sensor, (e) furnace, (f) pump, (g) gas tank, (h) microcomputer, (i) interface, (j) video monitor, (k) printer/plotter, (1) temperature sensor input, (2) pressure sensor input, (3) furnace power supply, (4) sensor power supply, (V1–V3) valves.

earlier in $Nd_2Fe_{14}B$ [13]. Stage I hydrogen adsorption occurs at about 250° C. On cooling (Segment CF in Fig. 2) the sample is found to retain the Th_2Zn_{17} structure with increased lattice parameters, listed in Table I. Under these conditions the hydrogen content in the formula $R_2Fe_{17}H_y$ is typically $y = 2.2$. The increase in volume $\Delta V/V = 2.8$ to 2.9% corresponds to an extra volume per absorbed hydrogen of $0.0034\,nm^3$, which is in fair agreement with the generally observed value of $0.0029\,nm^3$ per atom ($3.8\,cm^3\,mol^{-1}$) [14]. A differential scanning calorimetry (DSC) trace of the rhombohedral $Nd_2Fe_{17}H_{2.4}$ phase is shown in Fig. 3. The broad exothermic peak at 350° C corresponds to hydrogen desorption. Near 600° C the sample reabsorbs a large amount of hydrogen (Segment DE in Fig. 2). This Stage II absorption corresponds to decomposition of the material into $RH_{2-\varepsilon} + \alpha$-Fe. Mössbauer spectra described below for samples cooled along Segment EG confirm that α-Fe is then the only remaining iron-bearing phase. No iron hydride is stable under these conditions.

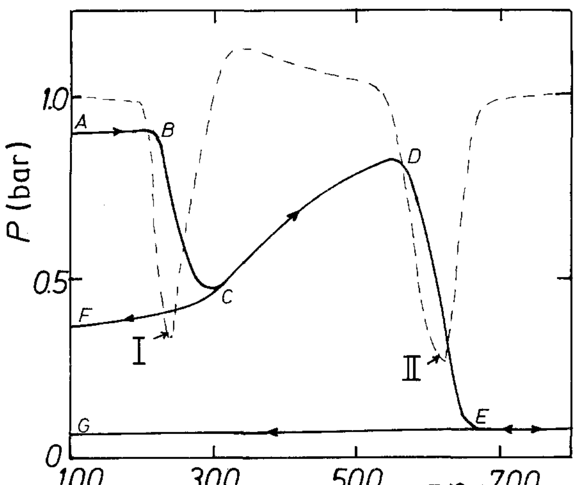

Figure 2 TPA trace for Nd_2Fe_{17} heated at $10°C\,min^{-1}$ showing the temperature dependence of (——) the hydrogen pressure and (– – –) its derivative dP/dT. Also included is the trace obtained on cooling from 300° C (C–F) and from 800° C (E–G). The two stages of hydrogen absorption are indicated by the arrows. $1\,bar = 10^5\,Pa$.

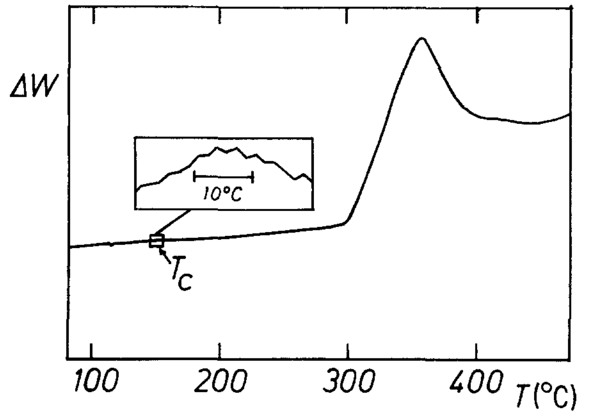

Figure 3 Differential scanning calorimetry (DSC) trace of $Nd_2Fe_{17}H_{2.4}$ heated in nitrogen at $20°C\,min^{-1}$.

3. Magnetic properties

The Curie temperature of the neodymium compound can be deduced from the small anomaly in the DSC trace (Fig. 3), but the hydrogenated samarium compound begins to lose its hydrogen before reaching T_c. Magnetic thermal scans were therefore carried out on samples of hydrogenated material sealed in very small double-walled quartz tubes with almost no free volume, so that hydrogen desorption is minimal. Typical results are shown in Fig. 4 and Table I, where it can be seen that T_c increases by well over 100° C for both rare earths. Curie temperatures of the unhydrogenated alloys are in good agreement with those reported in the literature [2].

Magnetization curves were then measured at 20° C using a vibrating-sample magnetometer. The results are shown in Fig. 5. The large increase in magnetization at this temperature ($\simeq 50\%$) essentially reflects the Curie temperature change.

Mössbauer spectra of both compounds were recorded at room temperature in the virgin state, in the hydrogenated state (Point F in Fig. 2) and in the decomposed state (Point G). The form of the spectra of the virgin samples is quite similar for samarium and neodymium [15] (Fig. 6). In the hydrogenated state there is a large increase in the hyperfine field, proportional to the increase in room-temperature magnetization. Average values are given in Table I. Mössbauer

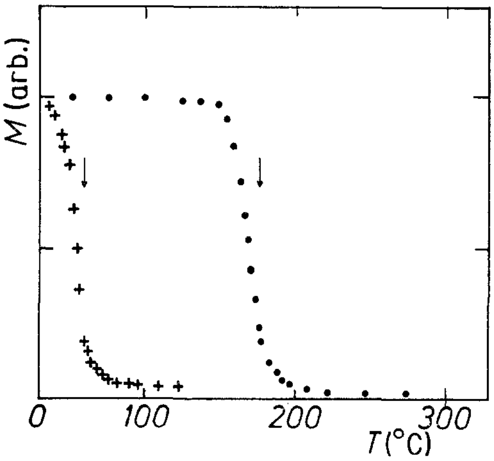

Figure 4 Temperature dependence of the magnetization of Nd_2Fe_{17} (+) before and (●) after hydrogenation to $Nd_2Fe_{17}H_{2.4}$.

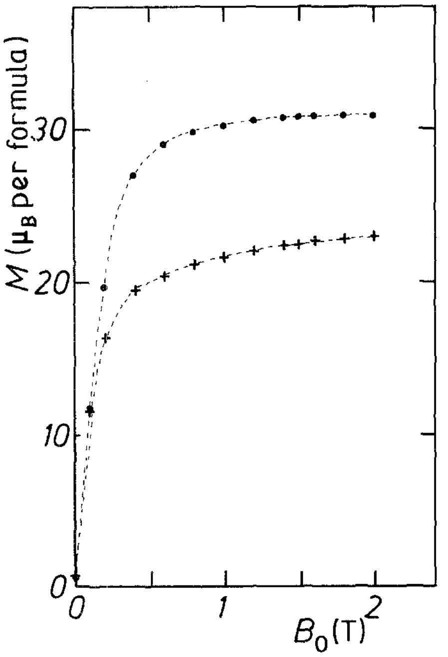

Figure 5 Room-temperature magnetization curves of Nd_2Fe_{17} (+) before and (●) after hydrogenation to $Nd_2Fe_{17}H_{2.4}$.

spectra of the decomposed samples show only iron metal.

4. Discussion

The hydrogenation behaviour of the R_2Fe_{17} phase is very similar to that of $R_2Fe_{14}B$ [12]. The same two-stage hydrogen absorption occurs, although the hydrogenation and decomposition temperatures are somewhat different. The Curie-temperature enhancement of Nd_2Fe_{17} is greater than that of $Nd_2Fe_{14}B$, although the absolute value remains lower. Thus, it appears that despite the increase of the rather weak ferromagnetic coupling in Nd_2Fe_{17}, it still remains less than that in $Nd_2Fe_{14}B$. The same mechanism of exchange enhancement, related to an increase in average Fe–Fe distances, seems to operate here as it does in $R_2Fe_{14}B$ [6] and iron-rich amorphous Fe_xM_{100-x} with $x \simeq 90$ and M = Y [4, 5], Zr [17] and Hf [16]. However, there may also be some significant increase in the electron density of states with hydrogen, as reported for $Fe_{88}Y_{12}H_x$ [5].

The anisotropy of the neodymium and iron sublattices in Nd_2Fe_{17} both favour the basal plane of the hexagonal structure, so even if the Curie temperature was higher, there would be no prospect of using the compound to make a permanent magnet. The magnetization in Sm_2Fe_{17}, however, may be expected to lie along the *c* axis, at least at low temperatures where the net axial anisotropy of samarium should outweigh the planar anisotropy of the iron sublattice. We observed no sign of axial anisotropy, however, in X-ray diffraction patterns or Mössbauer spectra of samples which were magnetically aligned at 20° C. Nevertheless, a small coercivity was found in both the virgin and hydrogenated Sm_2Fe_{17} materials, and work is continuing in this area.

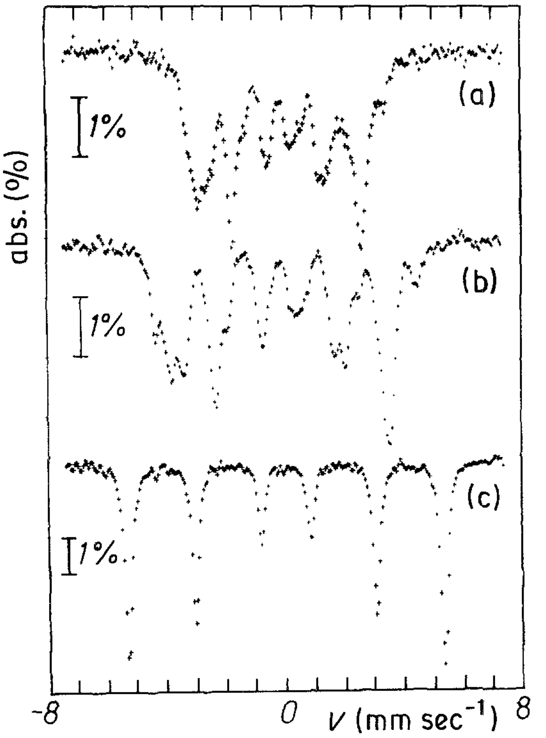

Figure 6 Mössbauer spectra of the Nd_2Fe_{17} (a) in the virgin state, (b) after Stage I hydrogenation and (c) after Stage II hydrogenation.

Acknowledgements

This work forms part of the Concerted European Action on Magnets, a project supported by the Stimulation Programme of the European Commission.

References

1. K. H. J. BUSCHOW, *Rep. Prog. Phys.* **40** (1977) 1179.
2. W. E. WALLACE, *Prog. Solid State Chem.* **16** (1985) 127.
3. K. H. J. BUSCHOW, M. BROUHA, W. J. M. BIESTERBOS and A. G. DIRKS, *Physica* **91B** (1977) 261.
4. J. M. D. COEY, D. RYAN, D. GIGNOUX, A. LIENARD and J. P. REBOUILLAT, *J. Appl. Phys.* **53** (1982) 7804.
5. J. M. D. COEY, A. LIÉNARD, J. P. REBOUILLAT, D. H. RYAN, WANG ZHENXI and YU BOLIANG, *J. Phys. F* **18** (1988) in press.
6. J. M. D. COEY, A. YAOUANC and D. FRUCHART, *Solid State Commun.* **58** (1986) 413.
7. P. l'HERITIER, P. CHAUDOUET, R. MADAR, A. ROUALT, J. P. SÉNATEUR and R. FRUCHART, *C. R. Acad. Sci.* **299 II** (1984) 849.
8. K. OESTERREICHER and H. OESTERREICHER, *Phys. Status Solidi* **A85** (1984) K61.
9. P. DALMAS de REOTIER, D. FRUCHART, L. PONTONNIER, F. VAILLANT, P. WOLFERS, A. YAOUANC, J. M. D. COEY, R. FRUCHART and P. l'HERITIER, *J. Less-Common Metals* **129** (1987) 133.
10. J. EVANS, C. E. KING and I. R. HARRIS, *J. Mater. Sci.* **20** (1985) 817.
11. A. E. RAY, *Acta Crystallogr.* **21** (1966) 426.
12. D. H. RYAN and J. M. D. COEY, *J. Phys. E* **19** (1986) 693.
13. J. M. CADOGAN and J. M. D. COEY, *Appl. Phys. Lett.* **48** (1986) 442.
14. H. PEISL, in "Hydrogen in Metals I", edited by G. Alefeld and J. Völkl, (Springer, 1978) p. 53.
15. P. C. M. GUBBENS, J. J. Van LOEF and K. H. J. BUSCHOW, *J. de Phys. Coll.* **35** (1974) C6–617.
16. D. H. RYAN, J. M. D. COEY and J. O. STROM-OLSEN, *J. Mag. Magn. Mater.* **67** (1987) 148.
17. D. H. RYAN, J. M. D. COEY, E. BATELLA, Z. ALTOUNIAN and J. O. STROM-OLSEN, *Phys. Rev. B* **35** (1987) 8630.

Received 1 April
and accepted 10 April 1987